Hindawi
Geofluids
Volume 2020, Article ID 2854187, 9 pages
https://doi.org/10.1155/2020/2854187

Research Article

Relationship between Movement Laws of the Overlaying Strata and Time Space of the Mined-Out Volume

Xiang Yu,[1] Kang Zhao ,[1,2] Qing Wang ,[1] Yajing Yan,[1] Yongjun Zhang,[3] and Junqiang Wang[2]

[1]*School of Architectural and Surveying & Mapping Engineering, Jiangxi University of Science and Technology, Ganzhou 341000, China*
[2]*Lingbao Jinyuan Mining Company Limited, Lingbao 472500, China*
[3]*School of Civil Engineering, Qingdao Technological University, Qingdao 266033, China*

Correspondence should be addressed to Kang Zhao; zhaok_666666@163.com and Qing Wang; wangqsvip@163.com

Received 6 August 2019; Revised 2 January 2020; Accepted 6 February 2020; Published 27 March 2020

Guest Editor: Glenda Taddia

The study and accurate prediction of the movement of overburden rock mass and surface subsidence are crucial for a safe production in metal mines. This study investigates the relationship between the movement laws of overlaying strata and the time space of a mined-out volume using Rock Failure Process Analysis (RFPA) System. Furthermore, the movement, deformation, and failure laws of overlaying strata are examined in different positions when a goaf volume is certain and the failure behavior of the overlaying strata. This study analyzes the similarities and differences of the overlaying strata comparatively. Results show that, regardless of the movement range or subsidence value of the overlying rock mass, a power function relationship is observed between them and working face advancement. Setting the equation shows that the scope of the overlying rock mass is significant when the ratio of a certain position distance roof to the working face distance is small. The results provide a reference for controlling the displacement of the overlying rock mass and treating goaf.

1. Introduction

The 3D stress balance of surrounding rock is destroyed by underground mining and tunnel excavation [1, 2], which can easily cause overburden movement, surface subsidence, and even collapse [3]. The collapse of a work-out area can seriously threaten a safe production and adversely affect the surface buildings and environment [4]. Currently, overlaying strata movement theory mainly includes "three zones," key strata, plate, and masonry beam theories [5, 6]. The main methods include probability integral, numerical simulation, similar model, stochastic medium, and neural network prediction [7–9]. Many studies on the coal seam movement with a satisfied application are available [10, 11]. The mining subsidence mechanism of a metal mine with fractured blocky rock mass is different from a coal mine with a layered rock mass. The rock mass in a metal mine has a typical inhomogeneous and discontinuous self-stressed block-hierarchical structure because the morphology of ore body, geological structure, and mining methods in metal mines differ from those in coal mines [12, 13]. The subsidence of overlaying strata in a metal mine is abrupt, and its subsidence, such as collapse pit and tubular or funnel collapse, is discontinuous. However, coal mine subsidence changes quite slowly [14, 15]. Thus, applying the movement theories of coal strata to metal mines is unsuitable. Consequently, investigating the overburden movement mechanism of metal mines is crucial.

At present, domestic and international scholars have created numerous theories and experience studies on overlaying strata movement from different angles and have gained certain achievements [16–20]. However, research on the time space of a mined-cavity volume based on the movement laws of overlaying strata is limited. On the basis of certain references [21], the stability of overlaying strata in metal mining has been analyzed systemically through a numerical simulation using rock mass failure process analysis software Rock Failure Process Analysis (RFPA) System [22, 23]. From the angle of quantitative analysis, the characteristics of the metal

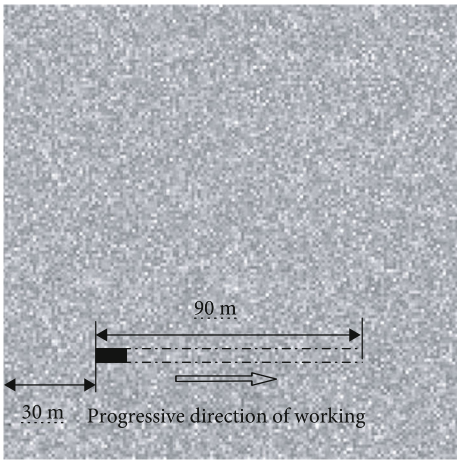

FIGURE 1: Calculation model.

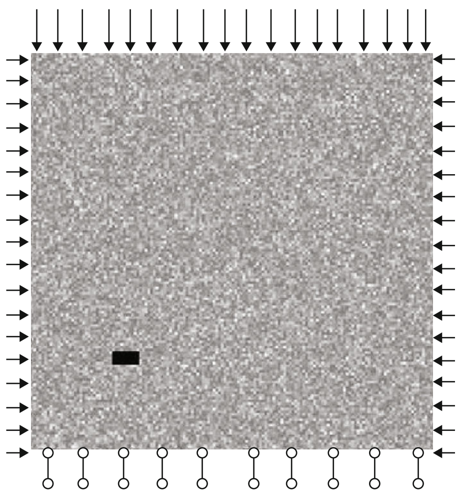

FIGURE 2: Mechanical model.

mine strata movement are investigated, and the formula between the overlying rock mass movement and the working face propulsion in different positions of goaves is obtained. This formula offers a new method for calculating the overlying rock mass movement.

2. Model Building and Parameter Setting

Based on a practical engineering [21], a gold metal mining has a background of a 500 m ore body depth, a dip near the horizontal, an ore body thickness near 5 m, and a 90 m ore body length. The region is mainly composed of silty clay and detritus. The overlaying strata contain few crush zones. The occurrence is steady, and the structure is simple, that is, its roof comprises sandy clay and shale with few mudstones, and the bottom consists of sandy clay and shale. This study investigates the failure process of an overlying rock mass by using a plane strain model. The calculation model is located 150 m along the horizontal direction, 150 m in the vertical direction, has a 5 m ore body thickness, an ore body that is 35 m from the lower boundary, and 30 m far from the left and right boundaries. The model is illustrated in Figures 1 and 2. The gravity stress function in the vertical direction and the model size are considered. Therefore, a 7 MPa stress must be applied to the vertical direction. According to the measured geostress data, a 2 MPa stress is applied to the horizontal direction combined with the geological features and tectonic stress in the mine. The model parameters are randomly assigned, in which an elasticity modulus is averaged, and other physical parameters are set in accordance with the mechanical properties of rocks to simulate the complexity of the geological occurrence conditions of metal mines accurately. The parameter is illustrated in Tables 1 and 2. Research on a dynamic damage rule of overlying rock mass under the condition of the ore mining process is conducted by using a step-by-step excavation model, and each step is 10 m.

3. Result Analysis of Overlaying Strata Failure

A goaf roof generates microcracks and sporadic caving before the working face advances to 50 m. Evident microfissure, propagation, and partially sporadic collapses are observed on the roof when the working face advances to 50 m, which has a 5 m length and arch shape. The result is shown in Figures 3 and 4. The rupture continues to expand and cause periodic caving with the increase in the mined-out volume. After the end of mining, the overlying rock mass no longer collapses, and only sporadic caving appears above the roof. The appearance of cracks in the interior of the overburden rock does not continue its connection, thereby indicating the inexistence of a large collapse area inside the overburden rock, but the plastic zone continues to expand.

This section investigates the strata displacement and deformation in different positions through a quantitative analysis. We monitored different positions in the overlaying strata (i.e., 5, 10, 20, 30, 50, and 80 m away from the roof) to investigate the displacement and deformation in the process of mining damage in different positions of the overlying rock mass. Given the proportion relationship between the ore body trend, mining length, and average mining depth, this study investigates the laws of overburden movement and failure of metal mines under the condition of nonfull mining.

Figure 5(a) illustrates the relationship among displacement changes with a 5 m distance from the roof in the overlaying strata and working face advancement. The results showed that the range of the work-out area increases with the working face length. The subsidence range of rock mass, which has a 5 m distance from the roof, is gradually increased. The subsidence process of the overlying rock mass gradually changes before the working face advances to 40 m. The overlying rock mass displacement is small. Thus, a slight mutation has occurred, thus indicating that a small amount of rupture occurs in the rock material, and the change in the overlying rock displacement is limited given the change in the volume of the rock material molecule itself. Figure 5(a) also demonstrates that the maximum subsidence value is 2.17 mm, and the sinking range is 20 mm when the working face advances to 10 m. The maximum subsidence value is 12.03 mm, and the sinking range is approximately 20 mm when the working face advances to 30 m. All of these observations indicate that no major failure and coalescence

Table 1: Boundary condition and mining parameter.

Control condition	X direction stress	Simulation tectonic stress	2 MPa	Load type	Plane strain
	Y direction stress	Overlaying rock mass gravity	7 MPa	Strength criterion	Mohr-Coulomb criterion
Simulation mining	Ore body distance from upper boundary (m)	110	Working thickness (m)	5	
	Each step mining long (m)	10	Total mining step/step	9	

Table 2: Physical-mechanical parameters of the model.

Rock type	Elasticity modulus (MPa)	Uniaxial compressive strength (MPa)	Bulk density (kN/m^3)	Poisson ratio	Internal friction (°)
Sandy stone	10000	90	25	0.25	30
Shale	15000	100	28	0.24	35
Siltstone	5000	20	22	0.3	30
Mudstone	2000	10	20	0.3	25
Silty clay and detritus	1000	2	14	0.35	20

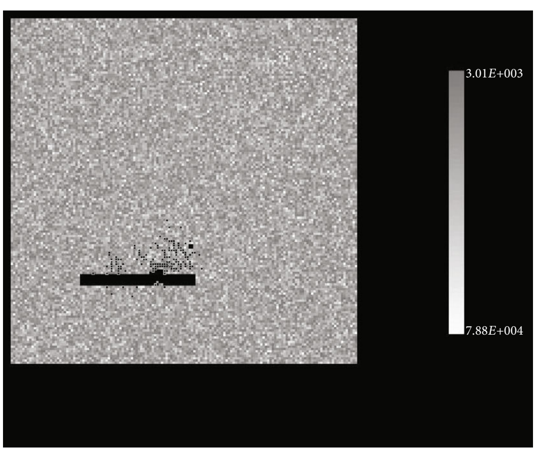

Figure 3: Breaking conditions in the roof.

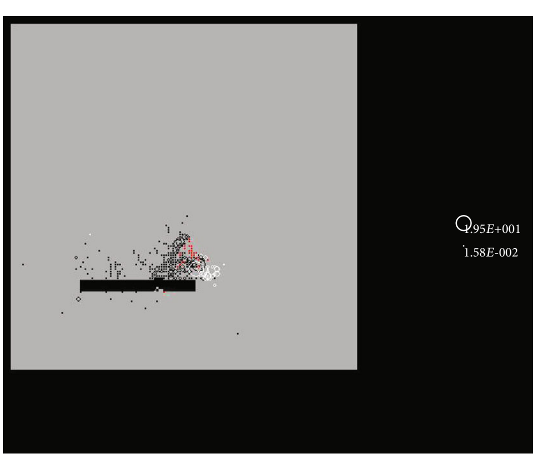

Figure 4: Acoustic emission distribution.

occur in the overlying rock mass. When the working face advances to 40 and 50 m, the subsidence curve shows a mutation trend, especially when the working face advances to 50 m. A “sharp point” in the curve is observed, and the maximum subsidence reaches 34.32 mm. The result shows that the overburden rock material itself has numerous molecular damages. Furthermore, crack coalescence and interaction may induce mutation. The subsidence curve has been interrupted in the working face between 60 and 90 m, thereby indicating that the collapse occurs 5 m away from the roof. The subsidence range increases with the advancement in the working face. Overall, the large subsidence and abrupt change in the overburden are caused by fissures and coalescence inside the overlying rock mass.

Figure 5(b) depicts the relationship between displacement change with a 10 m distance from the roof in the overlaying strata and the working face advancement. The range value of subsidence in the 5 m overlying distance from the roof increases with the advancement in the working face. When the working face advances to 50 m, the subsidence curve is gradual, thus implying that the overlying rock has not resulted in a hole-through crack, and the failure and movement of the rock material produce a large displacement. This phenomenon denotes that no collapse occurs in the overlaying strata. The subsidence curve is interrupted when the working face advances from 60 m to 90 m, thereby signifying an occurrence of a collapse. However, the interval of interruptions is smaller than that demonstrated Figure 5(a). When the working face advances to 60 m, the caving length becomes 10 and 20 m with 10 and 5 m distance from the roof, correspondingly. When the working face advances to 90 m, the caving length becomes 11 and 22 mm with 10 and 5 mm distance from the roof, respectively. The strata subsidence is smaller at 10 m than at 5 m.

Figure 5(c) exhibits that the range and value of the overlying rock mass subsidence, which are 20 m away from the roof, increase with the advancement in the working face.

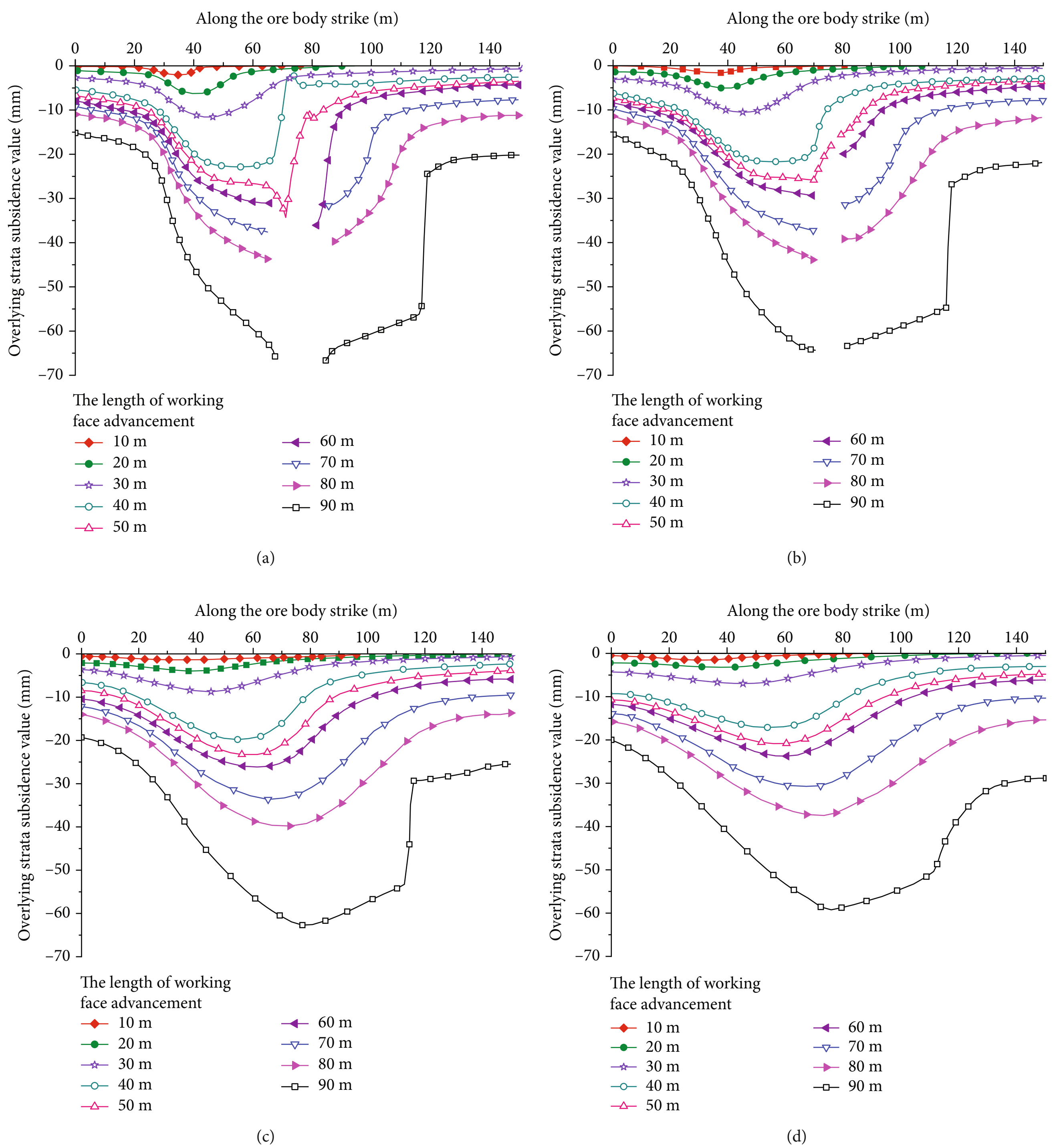

FIGURE 5: Continued.

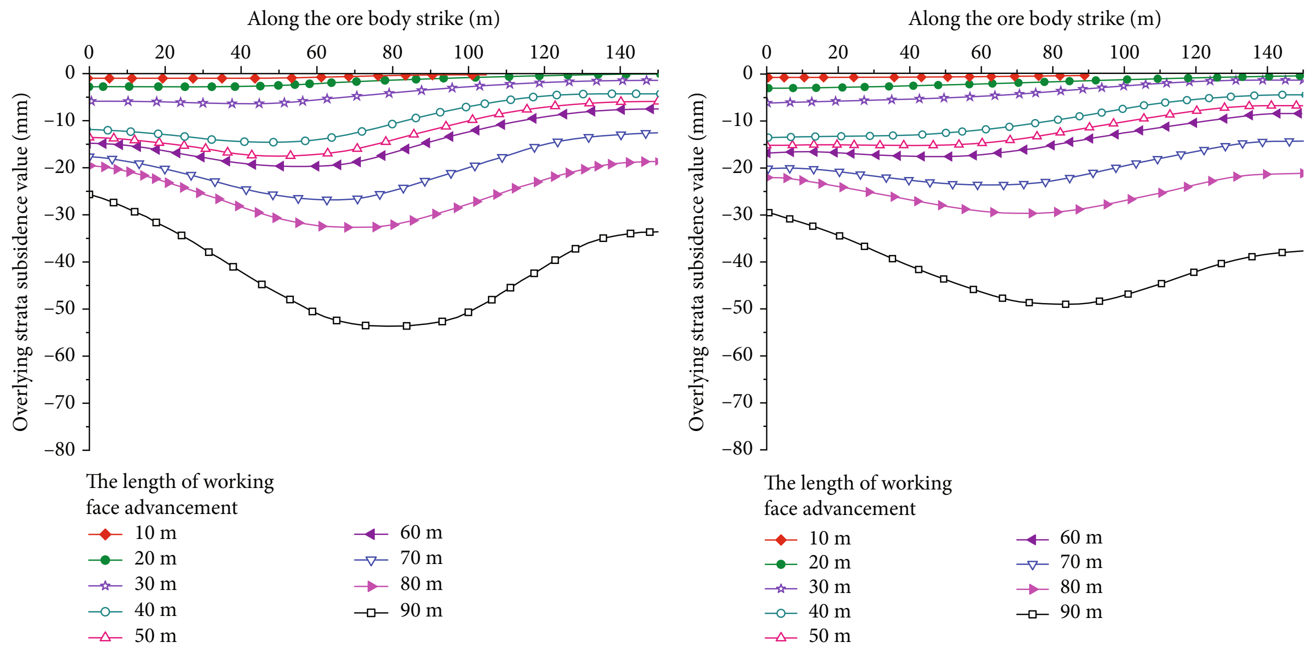

(e) (f)

Figure 5: (a) Distance to roof 5 m. (b) Distance to roof 10 m. (c) Distance to roof 20 m. (d) Distance to roof 30 m. (e) Distance to roof 50 m. (f) Distance to roof 80 m.

Furthermore, the strata subsidence curve gradually changes. Thus, the internal material of the rock cover does not produce large fracture and caving before the working face advances to 80 m. The sinking curve is continuous until the working face advances to 90 m. Moreover, a polyline is produced, thereby indicating that the rock cover's internal material fracture and the longevity of a small displacement are insufficient for fracture and caving. At this time, the maximum subsidence value reaches 62.82 mm, which is the tipping point of the caving area.

Figure 5(d) displays the relationship between the displacement change with a 30 m distance from the roof in the overlaying strata and the working face advancement. The range and value of subsidence in the overlaying strata with a 50 m distance from the roof gradually increase with the advancement in the working face. Although the subsidence curve, as a whole, is continuous, the curve is smoother than that with the 20 m distance from the roof. This finding shows the absence of microfissures in the overlying rock mass, but a few materials inside the damage still exist, thereby locally affecting its sinking displacement. The maximum sinking amount at this time is 58.83 mm.

Figure 5(e) presents the relationship between the displacement change with a 50 m distance from the roof in the overlaying strata and the working face advancement. With the advancement in the working face, the range and value of subsidence with a 50 m distance from the roof in the overlying rock mass gradually increase. Figure 5(e) also illustrates that the subsidence curve of the overburden rock is smooth, thereby indicating no large fissure zone in the overlying rock at 50 m from the top of the roof from the beginning to the end of ore body mining. Moreover, the fracture is only found inside the material, thereby denoting that the area belongs to the plastic zone. The acoustic emission and overburden rock burst figure in this region do not exhibit a large rupture, and an acoustic emission gathers nucleation. In the end, the ore body mining subsidence is 53.46 mm.

Figure 5(f) demonstrates that the subsidence curve is linear 80 m away from the roof before the working face advances to 80 m, thereby implying that this area is elastic. A minimal acoustic emission signal indicates the occurrence of a slight rupture inside the rock material. The subsidence curve has a downward bending trend, thus indicating that several material molecules have been destroyed at this time. The overlaying strata can produce a small displacement and a maximum subsidence value of 48.71 mm, which denotes a plastic region.

The aforementioned diagrams depict the following laws of overburden failure and displacement through vertical and horizontal comparison.

Therefore, we can analyze and draw the following conclusions in a certain position in the overlaying strata: the subsidence value and movement range of an overlying rock mass gradually increase with the advancement in the working face. The maximum subsidence vertex curve gradually moves toward the direction of the working face advancement.

Furthermore, we can analyze and draw the following conclusions when the working face advancement is certain: the subsidence value and movement range of an overlying rock mass decrease with the increase in the distance to the roof. The slope changes in the subsidence curve vertices reflect the rate of subsidence value change at a definite localization. The subsidence value and rate of change are large when the slope variation is also considerable. The

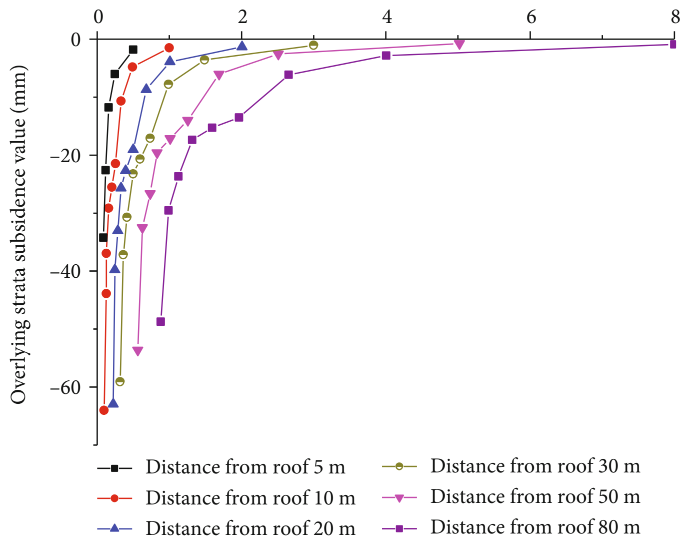

Figure 6: Relationship subsidence and ratio of distance to roof and working face advancement.

Table 3: Ratio of subsidence to working face advancement.

Distance from roof (m)	Coefficient a	Coefficient b	Correlation coefficient R^2
5	-0.52	-1.83	
10	-1.94	-1.56	
20	-4.24	-1.72	
30	-7.19	-1.82	0.97
50	-14.86	-2.03	
80	-34.57	-1.98	
Average value	-10.55	-1.82	

interruption in the curve reflects the occurrence of collapse in this area. The horizontal distance of the interruption indicates the size of the caving area. Under the condition of the same working face length, a high horizontal distance of the interruption indicates that the gob roof is near, and the collapse area is large.

4. Function Building and Discussion

Figure 6 exhibits the ratio relation between the subsidence value in the different positions in the overlaying strata and the working face length to investigate the relationship between the subsidence and the movement range in different overlying rock mass positions. In accordance with the fitted curves under different conditions, the models of the working face distance and subsidence in the various positions of the overlaying strata are established. The power function relationship between different position subsidence and overlaying strata is evident. Power function can be expressed as $y = ax^b$. The parameters are shown in Table 3.

Thus, the final curve equation can be represented as $y = 10.55x^{1.82}$.

A small ratio of the position distance from the roof to the overlaying strata and the working face advancement indicates a large subsidence by analyzing the curves and equations in Figure 7. When the ratio tends to 0, the subsidence tends to infinity. This result is consistent with the actual monitoring data. A collapse does not produce data, and the final subsidence amount cannot be monitored. A large ratio of the distance from a certain position to the gob roof and the working face advancement implies a considerable distance from the roof or a small mined-out volume and a small subsidence in the overlaying strata. The overburden strata do not move when the position arrives at infinity or is not a goaf.

Figures 8 and 9 display the relationship between the overlaying strata movement range and the working face advancement. This relationship is similar to the laws of strata subsidence. A power function relationship between these factors is observed through data analysis. The equation can be expressed as $y = ax^b$. The parameters are shown in Table 4.

Thus, the final curve equation can be represented as $y = 28.19x^{1.14}$.

The results show that, when the ratio of the position distance roof to the working face is small, the scope of the strata movement is extensive. In particular, the overlying rock mass that is close to the roof or the relatively large gob volume can considerably influence the strata movement. The scope of the strata movement is small when the ratio of the distance to the roof and the working face is large. When infinity or no goaf is reached, the overlying rock does not move.

5. Conclusion

In a certain position in the overburden, the subsidence value and movement range of overburden rock gradually increase with the advancement in a working face (the volume of goaf increases gradually). The maximum subsidence vertices of a

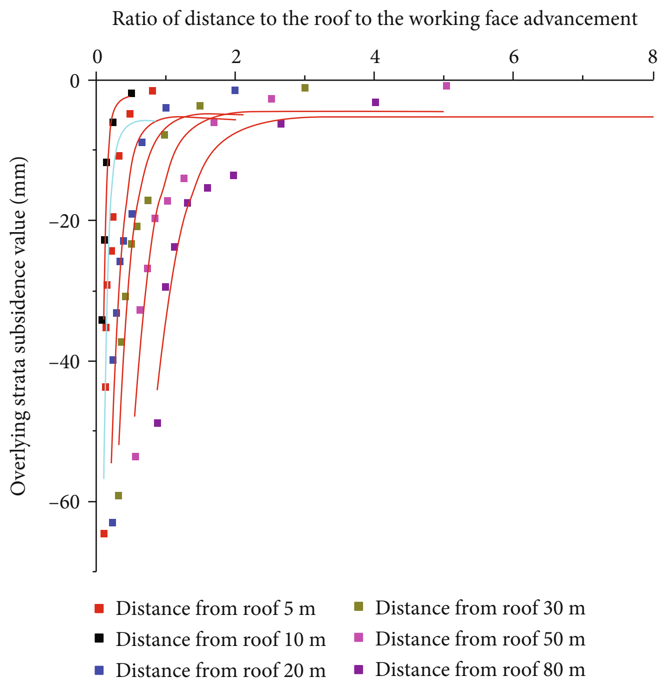

Figure 7: Fitting relationship subsidence and ratio of distance to roof and working face advancement.

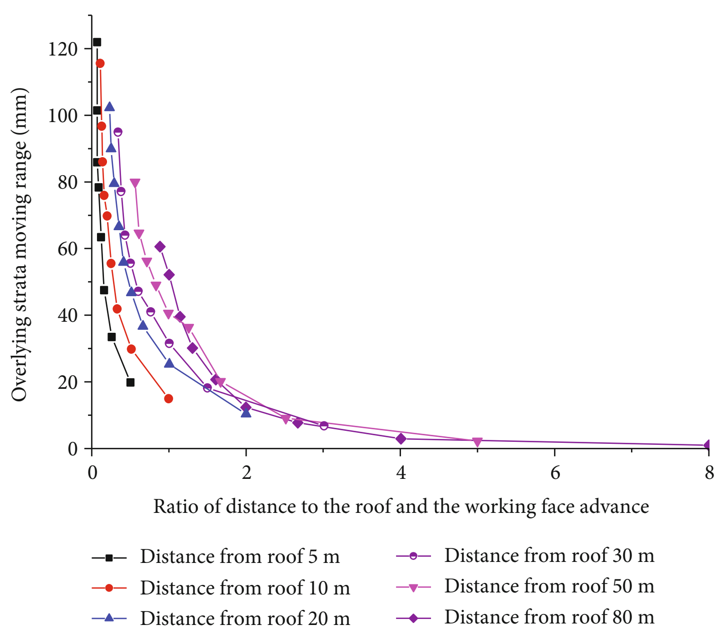

Figure 8: Relationship movement range and ratio of distance to roof and working face advancement.

curve gradually move toward the direction of the working face advancement.

(1) When the working face advancement is certain, the movement range and subsidence value have decreased with the increase in the monitoring of the distance to the roof. The subsidence curve breakpoints reflect a collapse in this area. The horizontal distance of the interruption indicates the size of the caving area. Under the condition of the same working face length, a high horizontal distance of the interruption that denotes a close roof indicates a large collapse area

(2) Regardless of the subsidence or movement range of the overlaying strata, all of subsidence or movement range and working face advancement perform the power function relationship ($y = ax^b$). The overlaying strata subsidence and working face advancement satisfy the power function relationship as follows: $y = 10.55x^{1.82}$. The overlaying strata movement range

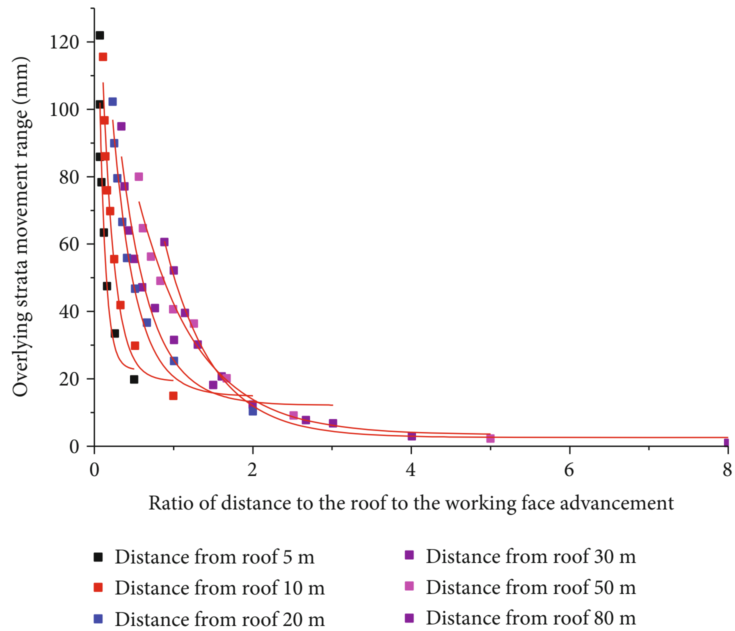

FIGURE 9: Fitting relationship movement range and ratio of distance to roof and working face advancement.

TABLE 4: Ratio of movement range to working face advancement.

Distance from roof (m)	Coefficient a	Coefficient b	Correlation coefficient R^2
5	10.28	-0.88	
10	16.11	-0.88	
20	24.29	-0.95	
30	28.60	-1.05	0.99
50	39.77	-1.16	
80	50.07	-1.9	
Average value	28.19	-1.14	

and working face advancement satisfy the power function relationship as follows: $y = 28.19x^{1.14}$

(3) The scope of the strata movement is extensive when the ratio of the position distance to the roof and the working face advancement is small. When the ratio of the position distance to the roof and the working face is large, the strata movement demonstrates a small scope. The overburden strata do not move when infinity or no gob is reached

Data Availability

The test data used to support the findings of this study are included within the article. Readers can obtain data supporting the research results from the test data table in the paper.

Conflicts of Interest

No conflict of interest exits in the submission of this manuscript, and manuscript is approved by all authors for publication. I would like to declare on behalf of my co-authors that the work described was original research that has not been published previously, and not under consideration for publication elsewhere, in whole or in part. All the authors listed have approved the manuscript that is enclosed.

Acknowledgments

The study has been supported by the National Natural Science Foundation (No. 51764013), by the Science and Technology Support Plan Project of Jiangxi Provincial Science and Technology Department (Grant No. 20161BBG70075, 20143ACG70010), by the Key Research Project of Science and Technology of Jiangxi Provincial Education Department (Grant No. GJJ160592), and by the Undergraduate Innovation and Entrepreneurship Training Program (Grant No. XS2018-S012). Sincere thanks are given to Dr. Shuai Cao for his technical guidance on this manuscript.

References

[1] W. A. Griffith, J. Becker, K. Cione, T. Miller, and E. Pan, "3D topographic stress perturbations and implications for ground control in underground coal mines," *International Journal of Rock Mechanics and Mining Sciences*, vol. 70, pp. 59–68, 2014.

[2] P. Wang, L. S. Jiang, P. Q. Zheng, G. P. Qin, and C. Zhang, "Inducing mode analysis of rock burst in fault-affected zone with a hard–thick stratum occurrence," *Environmental Earth Sciences*, vol. 78, no. 15, p. 467, 2019.

[3] S. J. Schatzel, C. Ö. Karacan, H. Dougherty, and G. V. R. Goodman, "An analysis of reservoir conditions and responses in longwall panel overburden during mining and its effect on gob gas well performance," *Engineering Geology*, vol. 127, pp. 65–74, 2012.

[4] E. F. Salmi, M. Nazem, and M. Karakus, “Numerical analysis of a large landslide induced by coal mining subsidence,” *Engineering Geology*, vol. 217, pp. 141–152, 2017.

[5] L. Jiang, P. Wang, P. Zheng, H. Luan, and C. Zhang, “Influence of Different Advancing Directions on Mining Effect Caused by a Fault,” *Advances in Civil Engineering*, vol. 2019, Article ID 7306850, 10 pages, 2019.

[6] J. Cheng, G. Zhao, and S. Li, “Predicting underground strata movements model with considering key strata effects,” *Geotechnical and Geological Engineering*, vol. 36, no. 1, pp. 621–640, 2018.

[7] T. N. Do, J. H. Wu, and H. M. Lin, “Investigation of sloped surface subsidence during inclined seam extraction in a jointed rock mass using discontinuous deformation analysis,” *International Journal of Geomechanics*, vol. 17, no. 8, article 04017021, 2017.

[8] Z. Yang, Z. C. Zhu, and H. J. Mi, “Numerical simulation research of wall rock stability of multi-stage excavated workings at Chengchao iron mine,” *Journal of Jiangxi University of Science and Technology*, vol. 34, pp. 34–40, 2013.

[9] B. Ghabraie, G. Ren, J. Smith, and L. Holden, “Application of 3D laser scanner, optical transducers and digital image processing techniques in physical modelling of mining-related strata movement,” *International Journal of Rock Mechanics and Mining Sciences*, vol. 80, pp. 219–230, 2015.

[10] R. Singh, P. K. Mandal, A. K. Singh, R. Kumar, J. Maiti, and A. K. Ghosh, “Upshot of strata movement during underground mining of a thick coal seam below hilly terrain,” *International Journal of Rock Mechanics and Mining Sciences*, vol. 45, no. 1, pp. 29–46, 2008.

[11] B. Unver and N. E. Yasitli, “Modelling of strata movement with a special reference to caving mechanism in thick seam coal mining,” *International Journal of Coal Geology*, vol. 66, no. 4, pp. 227–252, 2006.

[12] J. Rošer, D. Potočnik, and M. Vulić, “Analysis of dynamic surface subsidence at the underground coal mining site in Velenje, Slovenia through modified sigmoidal function,” *Minerals*, vol. 8, no. 2, p. 74, 2018.

[13] N. L. Grigorenko, D. V. Kamzolkin, and D. G. Pivovarchuk, “Optimization of open-pit mining by the gradient method,” *Computational Mathematics and Modeling*, vol. 27, no. 3, pp. 351–359, 2016.

[14] G. Ren, B. N. Whittaker, and D. J. Reddish, “Mining subsidence and displacement prediction using influence function methods for steep seams,” *Mining Science and Technology*, vol. 8, no. 3, pp. 235–251, 1989.

[15] A. Jaiswal and B. K. Shrivastva, “Stability analysis of the proposed hybrid method of partial extraction for underground coal mining,” *International Journal of Rock Mechanics and Mining Sciences*, vol. 52, pp. 103–111, 2012.

[16] K. Zhao, Q. Li, Y. Yan, K. Zhou, S. Gu, and S. Zhu, “Numerical Calculation Analysis of the Structural Stability of Cemented Fill under Different Cement-Sand Ratios and Concentration Conditions,” *Advances in Civil Engineering*, vol. 2018, Article ID 1260787, 9 pages, 2018.

[17] A. M. Suchowerska, R. S. Merifield, J. P. Carter, and J. Clausen, “Prediction of underground cavity roof collapse using the Hoek-Brown failure criterion,” *Computers and Geotechnics*, vol. 44, pp. 93–103, 2012.

[18] K. Zhao, K. Zhao, and L. Shi, “Collapsing height prediction of overburden rock mass at metal mine based on dimensional analysis,” *Rock and Soil Mechanics*, vol. 36, pp. 2012–2026, 2015.

[19] K. W. Mills, O. Garratt, B. G. Blacka, L. C. Daigle, A. C. Rippon, and R. J. Walker, “Measurement of shear movements in the overburden strata ahead of longwall mining,” *International Journal of Mining Science and Technology*, vol. 26, no. 1, pp. 97–102, 2016.

[20] K. Zhao, Q. Wang, S. Gu et al., “Mining scheme optimization and stope structural mechanic characteristics for a deep and large ore body,” *JOM*, vol. 71, no. 11, pp. 4180–4190, 2019.

[21] K. Zhao, Z. Guo, and Y. Zhang, “Dynamic simulation research of overburden strata failure characteristics and stress dependence of metal mine,” *Journal of Disaster Research*, vol. 10, no. 2, pp. 231–237, 2015.

[22] C. A. Tang and T. Xu, “Rock failure process analysis method (RFPA) for modeling coal strata movement,” *Advances in Coal Mine Ground Control*, pp. 345–377, 2017.

[23] C. A. Tang, H. Liu, P. K. K. Lee, Y. Tsui, and L. G. Tham, “Numerical studies of the influence of microstructure on rock failure in uniaxial compression – Part I: effect of heterogeneity,” *International Journal of Rock Mechanics and Mining Sciences*, vol. 37, no. 4, pp. 555–569, 2000.